



Synthesis of spin-labeled riboswitch RNAs using convertible nucleosides and DNA-catalyzed RNA ligation



Lea Büttner[†], Jan Seikowski[†], Katarzyna Wawrzyniak, Anne Ochmann, Claudia Höbartner^{*}

Research Group Nucleic Acid Chemistry, Max Planck Institute for Biophysical Chemistry, Am Fassberg 11, Göttingen 37077, Germany

ARTICLE INFO

Article history:

Available online 15 April 2013

Keywords:

Solid-phase synthesis
Convertible nucleoside
Spin label
RNA ligation
Deoxyribozyme
Riboswitch

ABSTRACT

Chemically stable nitroxide radicals that can be monitored by electron paramagnetic resonance (EPR) spectroscopy can provide information on structural and dynamic properties of functional RNA such as riboswitches. The convertible nucleoside approach is used to install 2,2,6,6-tetramethylpiperidin-1-oxyl (TEMPO) and 2,2,5,5-tetramethylpyrrolidin-1-oxyl (proxyl) labels at the exocyclic *N*⁴-amino group of cytidine and 2'-*O*-methylcytidine nucleotides in RNA. To obtain site-specifically labeled long riboswitch RNAs beyond the limit of solid-phase synthesis, we report the ligation of spin-labeled RNA using an *in vitro* selected deoxyribozyme as catalyst, and demonstrate the synthesis of TEMPO-labeled 53 nt SAM-III and 118 nt SAM-I riboswitch domains (SAM = *S*-adenosylmethionine).

© 2013 Elsevier Ltd. All rights reserved.

1. Introduction

The structural and functional diversity of RNA is impressively represented by the large number of different noncoding RNAs, that have been discovered and continue to be discovered in all forms of life.¹ Spectroscopic studies of RNA folding and interaction of RNA with proteins, metabolites and other small molecules play fundamental roles for elucidating mechanistic principles of RNA function. Biophysical techniques that are based on fluorescence or EPR spectroscopy require the site-specific installation of emissive or paramagnetic labels into the RNA of interest. A number of synthetic approaches are available to directly incorporate modifications or install desired probes post-synthetically on pre-functionalized RNA.² Prominent methods involve conjugation of fluorophores or spin labels via amide bond formation using activated esters and amino-modified nucleic acids, and recently also cycloaddition reactions between alkynes and azides (click chemistry).^{3,4} Spin labels have also been incorporated into RNA via Pd-catalyzed cross-coupling with halogenated nucleobases⁵ and via conjugation to phosphorothioate-modified RNA.⁶ Convertible nucleosides⁷ provide a well-established alternative to functionalization of RNA at the exocyclic amino groups of the nucleobases.⁸ Recently, the first example for synthesis of spin-labeled RNA using a nitroxide-modified nucleoside phosphoramidite was reported.⁹

A heavily investigated class of regulatory RNA elements are riboswitch RNAs that alter gene expression levels in response to

metabolite concentrations.^{10,11} The lengths of riboswitch domains that are used for biophysical studies aiming at understanding riboswitch mechanisms range from ~30 to ~150 nt,¹² and are mostly beyond the length that is easily achieved by solid-phase synthesis in one piece. Therefore, synthetic modified RNA fragments are enzymatically ligated to the desired full-length products.¹³ T4 DNA ligase and T4 RNA ligase have been successfully used to synthesize chemically modified riboswitch RNAs^{14–18} and numerous other large RNA targets, including for example ribozyme domains^{19–21} and snRNAs.²² To our knowledge, the ligation of nitroxide-labeled RNAs has not yet been reported. A potential reason may be the sensitivity of nitroxides to reduction, a known problem in EPR studies involving proteins,²³ especially when the most sensitive six-membered-ring nitroxide, 2,2,6,6-tetramethylpiperidin-1-oxyl (TEMPO) is employed. Nitroxide labels based on five-membered heterocycles, such as 2,2,5,5-tetramethylpyrrolidin-1-oxyl (proxyl) derivatives, are known to be more stable towards reduction.²⁴ Increasing the size of the geminal alkyl groups (ethyl instead of methyl) has been shown to increase the half-life of paramagnetic species in the presence of reductants.^{25,26} The stability of nitroxides has important implications for EPR spectroscopy of nucleic acids *in vivo*, which is an emerging field of research.^{27,28} With these and other recent advancements for EPR-spectroscopic investigations of biomolecules,^{29,30} the accessibility of long spin-labeled RNA is of general interest.

We report the synthesis of nitroxide-labeled RNA, carrying 2,2,6,6-tetramethylpiperidin-1-oxyl (TEMPO) or 2,2,5,5-tetramethylpyrrolidin-1-oxyl (proxyl) spin labels at the exocyclic amino group of cytidine and 2'-*O*-methylcytidine, resulting in four types of spin-labeled RNA (Fig. 1). Here, we expand our previous report⁸

* Corresponding author. Tel.: +49 551 201 1685; fax: +49 551 201 1680.

E-mail address: claudia.hoebartner@mpibpc.mpg.de (C. Höbartner).

[†] These authors contributed equally to this work.

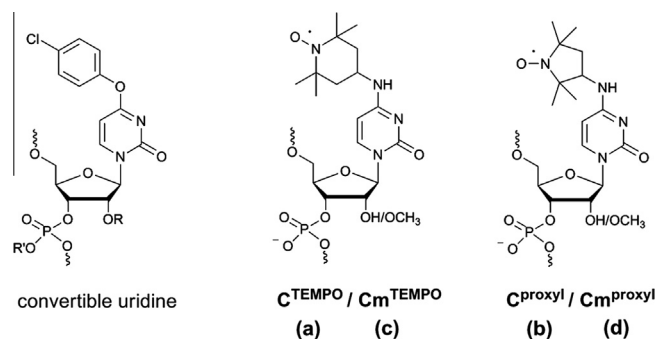


Figure 1. Convertible (4-chlorophenyl)uridine, TEMPO- and proxyl-labeled cytidine/2'-*O*-methylcytidine nucleotides in RNA. R = CH₃ or TOM, R' = 2-cyanoethyl.

on the installation of TEMPO groups on RNA using convertible nucleosides in solid-phase synthesis. In addition, we report *O*⁴-(4-chlorophenyl)-2'-*O*-methyluridine phosphoramidite that yields spin-labeled 2'-*O*-methyl-cytidine in RNA. The 2'-*O*-methyl group is a well-known RNA modification that is of natural importance and additionally has practical advantages due to the increased stability of modified RNAs.³¹ We examined and compared TEMPO- and proxyl-labeled RNAs by analysis of UV melting curves, and we characterized single-strand and duplex conformations by CW-EPR spectroscopy. Furthermore, we demonstrate efficient ligation of spin-labeled RNA by an optimized deoxyribozyme, as an alternative to protein-based RNA ligation.

Deoxyribozymes are artificial single-stranded DNAs of practical utility that are the result of *in vitro* selection experiments.^{32,33} The 9DB1 deoxyribozyme³⁴ catalyzes the formation of a native 3'-5' phosphodiester bond between two RNA fragments, by activating the 3'-hydroxyl group of the acceptor fragment for the nucleophilic attack at the alpha phosphate of a 5'-triphosphorylated donor fragment.³⁴ Recently we have identified the essential nucleotides in the catalytic core of the original 9DB1 DNA by combinatorial mutation interference analysis, and minimized the number of necessary nucleotides.³⁵ The shortened DNA 9DB1* is here used as a general

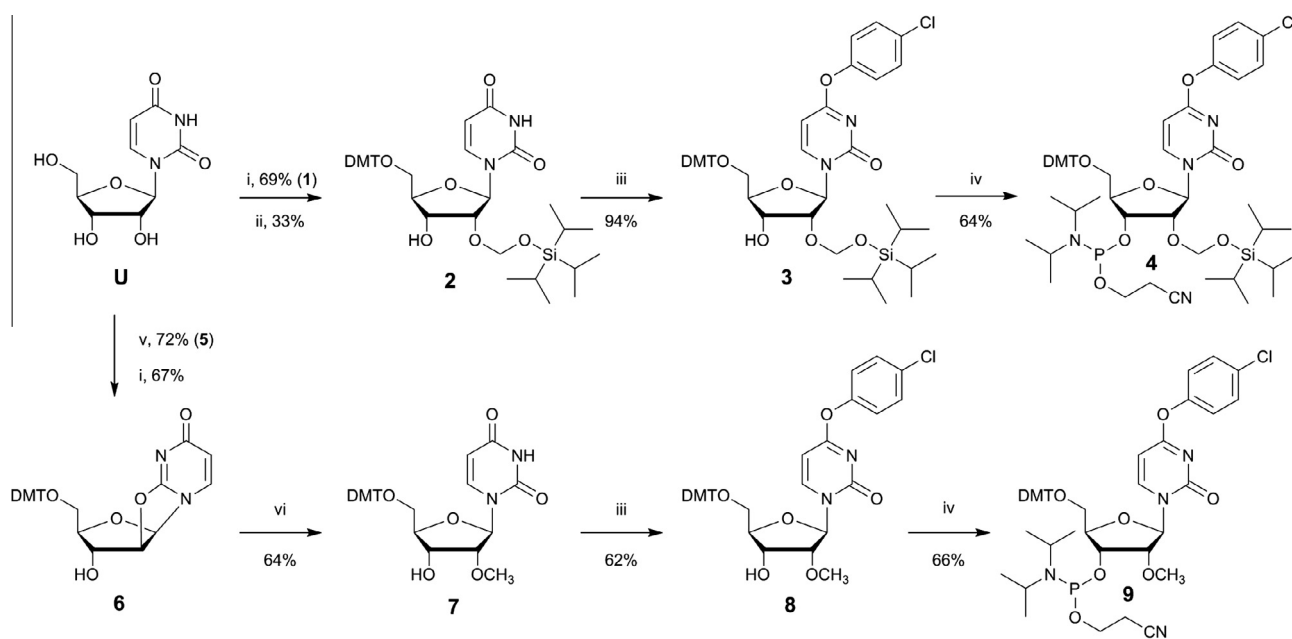
catalyst for the ligation of various spin-labeled and unmodified RNA substrates. We demonstrate five different systems, using RNA substrates in the lengths of 9–100 nt, resulting in ligation products of 26–118 nt. In particular, we synthesized spin-labeled variants of two riboswitch RNAs, SAM-I and SAM-III that bind the universal cofactor *S*-adenosylmethionine (SAM).

2. Results and discussion

2.1. Synthesis of convertible uridine phosphoramidites

Convertible nucleosides allow the functionalization of nucleobases at the exocyclic amino groups by displacement of appropriate leaving groups with alkylamines. The incorporation of *O*⁴-(4-chlorophenyl)uridine into RNA yields *N*⁴-modified cytidines in the final RNA.⁷ The 2'-*O*-tBDMS-protected phosphoramidite of *O*⁴-(4-chlorophenyl)uridine is commercially available, and has been employed successfully for the installation of TEMPO groups in RNA.⁸ Here we report an analogous convertible uridine building block that contains the (triisopropylsilyl)oxymethyl (TOM) group as alternative fluoride-labile 2'-protecting group. This permanent RNA protecting group offers advantages compared to tBDMS in terms of avoiding any issues related to potential 2',3'-isomerization and provides high coupling yields in shorter coupling times³⁶ (generally we use 4 min for TOM-protected phosphoramidites and 12 min for tBDMS-protected phosphoramidites).

The 2'-*O*-TOM-protected phosphoramidite **4** was synthesized in four steps from uridine, taking advantage of a late derivatization of the nucleobase (Scheme 1). The 5'-*O*-(4,4'-dimethoxytrityl) (DMT) group and the 2'-*O*-TOM groups were installed following reported procedures to yield nucleoside **2**.³⁶ The nucleobase was activated by formation of the *O*⁴-(2,4,6-triisopropylphenyl)sulfonyl (=trisyl) ester, which was not purified, and directly used in the next step. In the presence of *N,N*-dimethylethylamine and DBU, the sulfonyl ester was displaced with 4-chlorophenol to yield compound **3** in excellent yield. Intermediate protection of the free 3'-OH group was not necessary; the presence of bulky DMT and TOM groups and the large size of the trisyl group prevent any undesired side



Scheme 1. Synthesis of convertible uridine phosphoramidites **4** and **9**. Reagents and condition. (i), DMT-Cl, pyridine, 6 h, rt; (ii), (a) *n*Bu₂SnCl₂, *i*Pr₂NEt, (CH₂)₂, 45 min, rt, (b) TOM-Cl, 20 min, 80 °C; (iii), (a) trisyl-Cl, DMAP, NEt₃, CH₂Cl₂, 2 h, 0 °C-rt; (b) 4-chlorophenol, Me₂NEt, DBU, 3 h, rt; (iv) CEP-Cl, Me₂NEt, CH₂Cl₂, 2.5 h, rt; (v), Ph₂CO₃, NaHCO₃, DMF, 4 h, 120 °C; (vi), Mg(OCH₃)₂, DMF, 5 h, 100 °C.

reaction during sulfonylation. The 3'-OH was then functionalized using 2-cyanoethyl-(*N,N*-diisopropylamino) chlorophosphate (CEP-Cl) and *N,N*-dimethylethylamine in dichloromethane to give phosphoramidite **4**. Synthesis of the *O*⁴-(4-chlorophenyl)-2'-*O*-methyluridine phosphoramidite **9** was achieved along a similar route. Starting from uridine, 2,2'-*O*-anhydrouridine (**5**) was generated and converted to the 5'-*O*-DMT-protected compound **6** following reported procedures.^{37,38} Reaction with magnesium methoxide yielded nucleoside **7**,^{39,40} which was subjected to *O*⁴ activation as trisyl ester and derivatization with 4-chlorophenol. Without intermediate protection of the 3'-OH, the new compound **8** was obtained in respectable yield, and was then converted to 2-cyanoethyl *N,N*-diisopropyl phosphoramidite **9** upon reaction with CEP-Cl under established conditions.

2.2. Synthesis of spin-labeled RNA

The phosphoramidites **4** and **9** were used for solid-phase synthesis of RNA oligonucleotides on polystyrene support using 2'-*O*-TOM-protected RNA phosphoramidites, employing standard RNA coupling conditions and using *S*-benzylthiotetrazole (BTT) as activator. After complete assembly of the desired oligonucleotide sequence, the solid support was incubated with a 2 M solution of either 4-amino-TEMPO or 3-amino-proxyl in methanol at 42–55 °C for 24–48 h, followed by a short incubation with MeNH₂ or NH₄OH in H₂O for 2–5 h to remove remaining base-labile protecting groups (this step can be skipped for short TEMPO-labeled oligoribonucleotides with less than 15 nt, in which case the excess of amine is sufficient to cleave acyl and cyanoethyl groups). The 2'-protecting groups were removed with 1 M TBAF in THF, followed by desalting of the crude product and purification of the desired RNA by PAGE or anion exchange HPLC. The sequences of the synthesized spin-labeled oligonucleotides ranging from 9 to 27 nt are summarized in Table 1. In this manuscript, unmodified oligonucleotides are assigned with bold numbers. Modifications are indicated by lower case letters following the oligonucleotide number: **a** = **C**^{TEMPO}, **b** = **C**^{proxyl}, **c** = **Cm**^{TEMPO}, **d** = **Cm**^{proxyl} (Fig. 1). In addition to the nitroxide reagents, we have used 4-amino-2,2,6,6-tetramethylpiperidine (pip, letter **e** in oligo names) for substitution of *O*⁴-chlorophenyl uridine to prepare reference compounds for the stably reduced state of the TEMPO label (**19e** and **22e**).

Figure 2 displays examples for anion exchange HPLC profiles of crude and purified 15-mer RNAs **11c** and **11d** containing TEMPO- and proxyl-modified 2'-*O*-methylcytidine. The substitution with 4-amino-TEMPO was highly efficient and the desired TEMPO-labeled RNAs were produced as the major products in very good

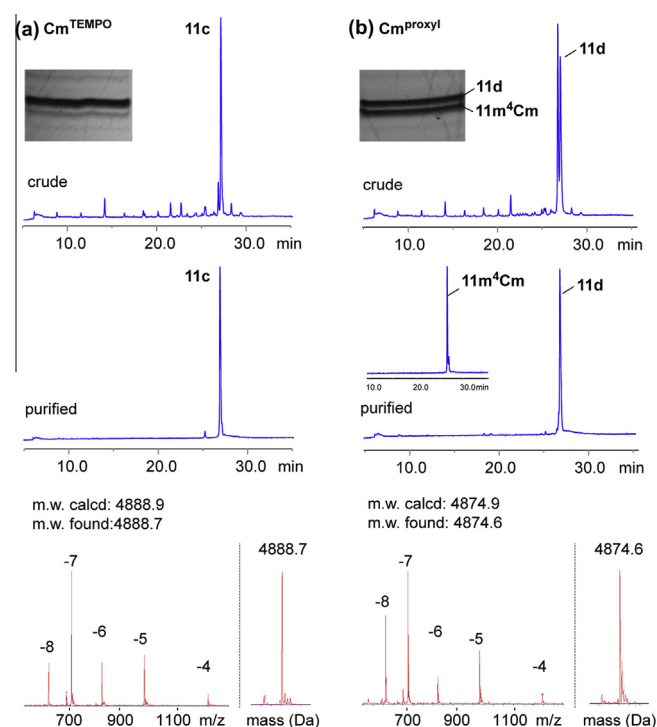


Figure 2. Synthesis, purification and analysis of spin-labeled RNA. (a) TEMPO-labeled 15-mer **11c**; (b) proxyl-labeled 15-mer **11d**. Anion exchange HPLC of crude and purified oligonucleotides, Dionex DNA-Pac PA200, 4 × 250 mm, 70 °C, 6 M urea, 0–48% in 12 CV. Denaturing polyacrylamide gel (7 M urea), 0.7 × 200 × 320 mm, 35 W. ESI-MS: raw spectrum (left) and deconvoluted mass spectrum (right, excerpt).

yield. In contrast, substitution with 3-amino-proxyl was generally less efficient; two products of about equal intensity were produced, which could be easily separated by denaturing polyacrylamide gel electrophoresis (see inset in Fig. 2b). The lower band (earlier eluting product on anion exchange column) was identified by ESI-MS as the *N*⁴-methylated derivative (*m*⁴Cm, *m*⁴C respectively), which originates from substitution of the *O*⁴-chlorophenyl group with MeNH₂. All spin-labeled RNAs were characterized by ESI-MS and the purity was checked by analytical anion-exchange HPLC (see supporting Figures S1–S3 for more examples).

2.3. Characterization of spin-labeled RNA by UV melting analysis and EPR spectroscopy

The influence of the TEMPO and proxyl spin labels on the thermodynamic stability of RNA duplexes was studied by analysis of UV melting curves. Three different lengths of RNA duplexes were investigated, containing 9, 15, or 20 base-pairs. The thermal melting results are summarized in Table 2, and melting curves for unmodified, TEMPO- and proxyl-labeled duplexes **11/11'** are depicted in Figure 3 and Figure S4. Thermodynamic parameters were extracted for the 15-mer duplexes **11/11'** by analyzing melting experiments at seven different concentrations (see Tables S3, S4, and Figure S5). All other duplexes were studied at least at two different RNA concentrations. The influence of the TEMPO and proxyl spin labels on the duplex stability is comparable; the TEMPO label is only minimally favored by a small difference of less than 1 °C (compare samples **a** with **b** and **c** with **d** in Table 2). The 2'-*O*-methyl group in samples **c/d** shows the expected small stabilizing effect compared to **a/b** for the 15 and 20 bp duplexes, but the influence on the 9 bp duplex is negligible. The drop in melting temperature compared to the unmodified RNA depends on the length of the duplex for all four modifications, and amounts to 8–9 °C for

Table 1
Modified RNA oligonucleotides

No	5'–Sequence–3'	m.w. calcd.	m.w. found
10a	GAC ^{TEMPO} GUCGGA	3047.8	3048.0
10b	GAC ^{proxyl} GUCGGA	3033.8	3033.4
10c	GACm ^{TEMPO} GUCGGA	3061.8	3061.3
10d	GACm ^{proxyl} GUCGGA	3047.8	3047.2
11a	AAGUC ^{TEMPO} UCAUGUACUA	4874.9	4874.8
11b	AAGUC ^{proxyl} UCAUGUACUA	4860.9	4860.3
11c	AAGUCm ^{TEMPO} UCAUGUACUA	4888.9	4888.7
11d	AAGUCm ^{proxyl} UCAUGUACUA	4874.9	4874.6
12a	GACGUC ^{TEMPO} GGAAGACGUCAGUA	6623.0	6624.0
12c	GACGUCm ^{TEMPO} GGAAGACGUCAGUA	6637.0	6637.8
19a	pAGAC ^{TEMPO} GUCAGUAp	3827.2	3827.0
19e	pAGAC ^{pip} GUCAGUAp	3812.2	3811.5
20a1	GUUC ^{TEMPO} CCGAAAGGAUGGUGGAAUCACCA	8849.3	8848.3
20a2	GUUCCGAAAGGAUGGUGGAAUC ^{TEMPO} ACCA	8849.3	8848.1
22a	UUCUUUAUC ^{TEMPO} AAGAGAAGCA	5878.5	5878.3
22e	UUCUUUAUC ^{pip} AAGAGAAGCA	5863.5	5863.6

Table 2
UV-melting analysis of spin-labeled RNA duplexes

No	Duplex	bp	C ^{TEMPO} (a)			C ^{proxyl} (b)		C ^{TEMPO} (c)		C ^{proxyl} (d)	
			T _m	T _m	ΔT _m ^a	T _m	ΔT _m	T _m	ΔT _m	T _m	ΔT _m
10	5' -GACGUCGGA-3'	9	57.0	48.7	-8.3	47.6	-9.4	48.6	-8.4	47.3	-9.7
10'	3' -CTGCAGCCT-5'										
11	5' -AAGUCUCAUGUACUA-3'	15	64.0	58.7	-5.3	57.9	-6.1	59.1	-4.9	58.4	-5.6
11'	3' -TTCAGAGTACATGAT-5'										
12	5' -GACGUCGGAAGACGUCAGUA-3'	20	82.3	76.7	-5.6	n.d.	-	77.4	-4.9	n.d.	-
12'	3' -CTGCAGCCTTCTGCAGTCAT-5'										

^aΔT_m = T_m(spin-labeled RNA) - T_m(unmodified RNA); in 10 mM potassium phosphate buffer, pH 7.0, 150 mM NaCl.

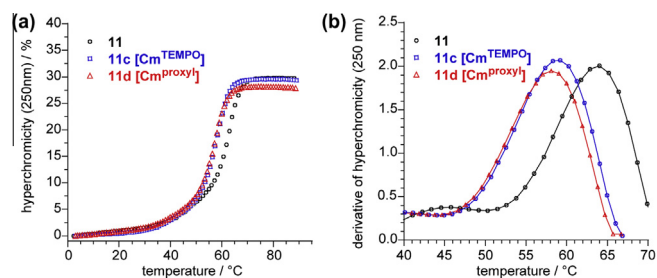


Figure 3. UV melting curves of spin-labeled RNA duplexes **11/11'**. 4 μM RNA, in 10 mM potassium phosphate buffer, pH 7.0, 150 mM NaCl. (a) Hyperchromicity at 250 nm, (b) derivative of hyp, maximum gives T_m.

the shortest 9 bp strands, and 5–6 °C for the samples containing 15 and 20 bp.

CW-EPR spectra were recorded to characterize the spin-labeled RNA oligonucleotides (Fig. 4 and Fig. S6), and to compare the relative mobility of the TEMPO and proxyl labels. The observed spectral broadening in the presence of the complementary strand confirms duplex formation. Compared to the non-base-paired situation in the single-strand, the overall dynamics of the spin label is reduced upon formation of a Watson–Crick base-pair between the labeled cytidine residue and guanosine in the complementary strand. The broader spectra for **11d** compared to **11c** suggest that the proxyl label is less mobile than the TEMPO label (see Fig. S6).

2.4. Ligation of short spin-labeled RNA

Using EPR to study longer RNAs than can be achieved by solid-phase synthesis requires ligation of modified RNA fragments. Here we employ the deoxyribozyme 9DB1* that catalyzes the formation

Table 3
Overview of RNA substrates and conditions for DNA-catalyzed ligation of spin-labeled RNA (spin-labeled nucleotides marked in red)

No	acceptor substrate 5'-sequence-3'	No	donor substrate 5'ppp-sequence-3'	product / length (nt)	9DB1	cond. ^a	see
10	GACGUCGGA	13	GAUCAAGUGUAGUAUCU	14 / 26	D1	C	Fig. S7
11	AAGUCUCAUGUACUA	15	GAUGUUCUAGCGCCGGA	16 / 32	D2	A	Fig. 4
12	GACGUCGGAAGACGUCAGUA	17	GACCUCGCAUCGUG	18 / 34	D3	B	Fig. 6
20	GUUCCCGAAAGGAUGGUGAAUCACCA	21	GAUGCCUUGUAACCGAAAGGGGAAU	SAM-III / 53	D4	A	Fig. 8
22	UUCUUAUCAAGAGAAGCA	23	GAGGGACUGGCCCGACGAAGCUUCAG CAACCGGUGUAAUGGCGAUCAGCCAU	24 / 70	D5	B	Fig. S10
22	UUCUUAUCAAGAGAAGCA	25	GAGGGACUGGCCCGACGAAGCUUCAG CAACCGGUGUAAUGGCGAUCAGCCAU GACCAAGGUGCUAAAUCAGCAAGCU CGAACAGCUUGGAAGAUAAGAA	SAM-I / 118	D5	B	Fig. 8, Fig. S11

^aCondition A: 40 mM Mg²⁺, pH 9.0, 37 °C, 5 h; B: 20 mM Mn²⁺, pH 7.5, 37 °C, 5 h; C: 20 mM Mn²⁺, pH 7.5, 25 °C, 15 h.

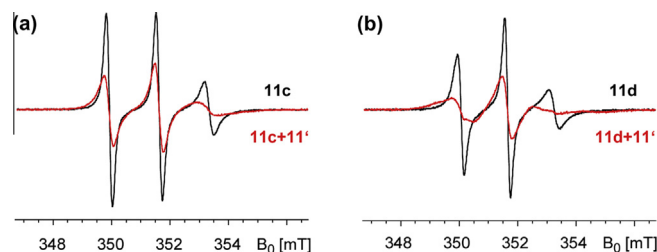


Figure 4. CW-EPR characterization of (a) TEMPO- and (b) proxyl-labeled RNAs **11** in single-strand (black) and duplex (red) in 2.5 mM potassium phosphate buffer, pH 7.0, 30 mM NaCl.

of a native 3'–5' phosphodiester bond between two RNA substrates for the ligation of spin-labeled oligonucleotides. We also compare the efficiency of DNA-catalyzed ligation with the traditionally used splinted ligation with T4 DNA ligase, and we study the fate of the spin-labeled species under ligation conditions and in the purified ligation product. Ligation experiments of spin-labeled RNAs are summarized in Table 3, the sequences of unmodified acceptor RNAs, 5'-activated donor RNAs, corresponding deoxyribozymes (D1–D5), and DNA splints are given in Tables S1 and S2.

The 9DB1* deoxyribozyme (Fig. 5a) hybridizes the RNA substrates via the 5' and 3' binding arms and uses the nucleotides of the catalytic core together with divalent metal ion cofactors to activate the 3'-OH group of the acceptor RNA for nucleophilic attack on the 5'-triphosphate of the donor RNA. Upon release of pyrophosphate, the native phosphodiester linkage is formed. The ligation sites for DNA-catalyzed RNA ligation were chosen based on the reported sequence preferences of 9DB1: the 3'-terminus of the acceptor RNA can be any nucleotide except C, and transcription of the donor RNA should be initiated with 5'-GA or 5'-AA (i.e., the sequence requirement is DJRA).³⁴

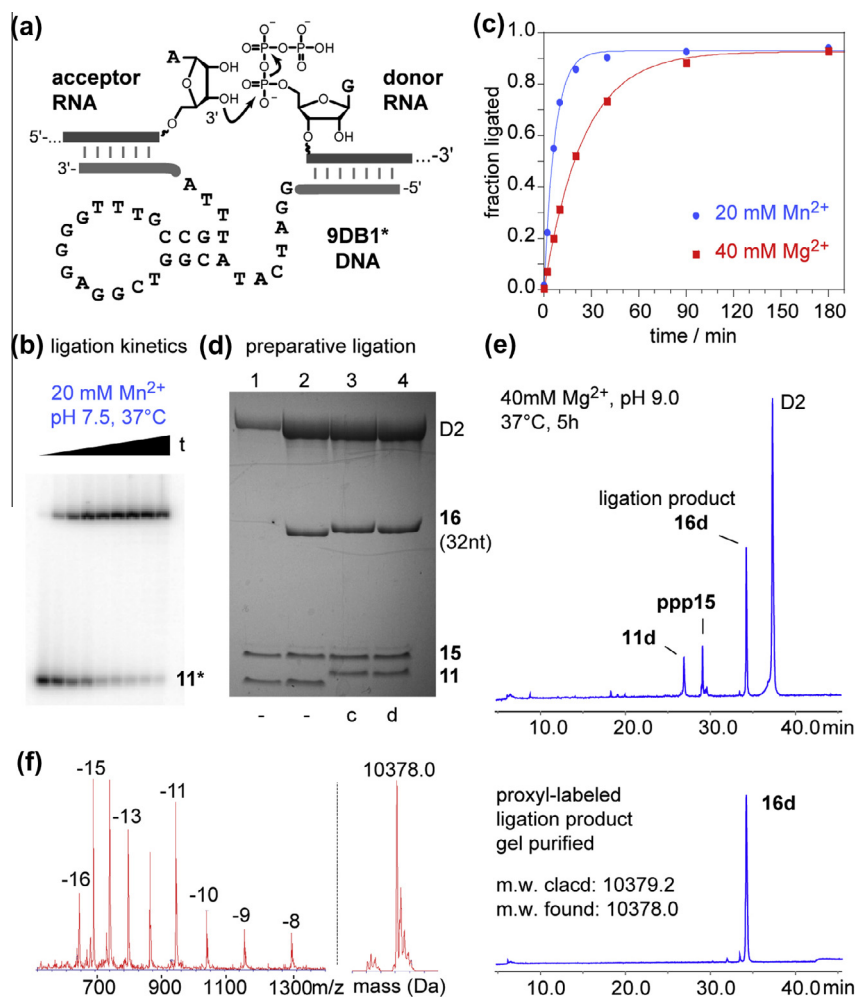


Figure 5. (a) Schematic depiction of RNA ligation by 9DB1* deoxyribozyme. (b) Analysis of ligation kinetics with Mn^{2+} as cofactor. (c) Kinetics plot (single-turnover conditions); $k_{obs}(Mn^{2+}) = 0.15 \text{ min}^{-1}$, $k_{obs}(Mg^{2+}) = 0.04 \text{ min}^{-1}$. (d) PAGE separation of ligation reactions **11**+**15** with 9DB1* DNA enzyme D2 (1.5 nmol scale). Lane 1. reference; lane 2. unmodified acceptor **11**; lane 3: Cm^{TEMPO} -labeled acceptor **11c**, lane 4: Cm^{proxyl} -labeled acceptor RNA **11d**. (e) Anion exchange HPLC analysis of ligation reaction after 5 h incubation time, and HPLC trace of gel-purified Cm^{proxyl} -labeled ligation product **16d** (isolated yield: 38%). (f) ESI-MS of **16d**.

The minimized deoxyribozyme 9DB1* used in this study resulted from combinatorial mutation interference analysis of the original sequence.³⁵ Upon continued studies on the mechanism of the DNA-catalyzed reaction, we found that Mn^{2+} at pH 7.5 leads to faster ligation compared to the originally reported conditions with Mg^{2+} at pH 9.0 (Fig. 5). For working with longer RNA substrates, the lower pH is an additional advantage. The ligations were scaled up and performed in parallel with unmodified and spin-labeled RNAs. In all studied cases involving RNAs **10**, **11** and **12**, the spin labels did not affect the reaction, and the paramagnetic products were isolated by denaturing PAGE, and characterized by HPLC, MS and CW-EPR.

Before studying 9DB1* for the ligation of spin-labeled RNA, we used traditional splinted ligation with T4 DNA ligase (or T4 RNA ligase) for connecting synthetic RNA fragments. However, using spin-labeled substrates, we faced the formation of a number of undesired byproducts which caused a reduced yield of the desired products. In addition, upon gel-purification, a small amount of a byproduct that elutes earlier on anion exchange HPLC could not be separated. This byproduct contained a reduced TEMPO substituent. In contrast, the ligation reaction with 9DB1* proceeded very cleanly and produced spin-labeled ligation product in high quality and good yield (Fig. 6, S7, S8).

To further investigate the problematic partial loss of spin label during protein-catalyzed ligation reactions, we compared the anal-

ysis of spin-labeled RNA after incubation with T4 DNA ligase buffer in contrast to deoxyribozyme ligation buffer (Fig. 7a). While the RNA was still intact after 5 h of incubation in the presence of 20 mM Mn^{2+} at pH 7.5, about 15% of the corresponding amine was produced in the presence of 10 mM DTT in the T4 DNA ligase buffer. In a second experiment, TEMPO-labeled RNA was incubated with 100 mM DTT in 10 mM Tris-HCl, pH 7.8 and analyzed by anion exchange HPLC (Fig. 7b). By comparison and co-injection (Fig. S9) with an authentic sample of 2,2,6,6-tetramethylpiperidine-substituted RNA it was confirmed that the undesired byproduct must have lost the nitroxide. T4 DNA ligase can also be used in a DTT-free reaction buffer, but the concentration of DTT that comes from the storage buffer of the enzyme was sufficient to complicate the purification of high-quality spin-labeled RNA. The instability of TEMPO groups in the presence of DTT is a known problem that has affected investigations of spin-labeled proteins.²³ The effect of DTT concentration on the intensity of the EPR signal has been reported, and tris(2-carboxyethyl)phosphine (TCEP) has been suggested as alternative sulfhydryl reductant that leads to reduced rate of TEMPO reduction.²³ Potentially TCEP could be applied in T4 DNA catalyzed reactions. However, the general applicability of the 9DB1* deoxyribozyme, as demonstrated here for several examples of spin-labeled RNAs of different lengths, offers an efficient and reductant-free alternative for enzymatic ligation of labeled RNAs.

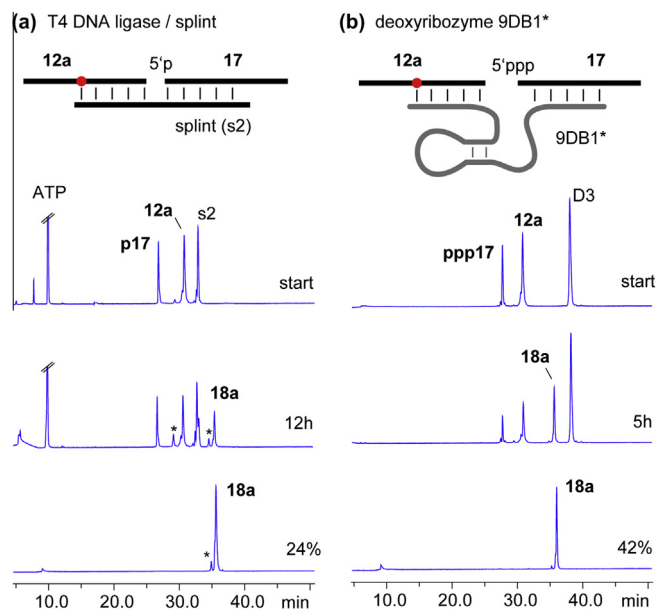


Figure 6. Comparison of protein- and DNA-catalyzed RNA ligation. (a) T4 DNA ligase mediated splinted ligation of C^{TEMPO}-labeled RNA **12a** and 5'-phosphorylated donor RNA **17**. Conditions: 15 μ M RNA, 40 mM Tris-HCl, pH 7.8, 10 mM MgCl₂, 10 mM DTT, 0.5 mM ATP, 37 °C, 12 h. (b) 9DB1*-catalyzed ligation of **12a** and 5'-triphosphorylated donor RNA **17**. Conditions: 15 μ M RNA, 20 mM MnCl₂, pH 7.5, 150 mM NaCl, 2 mM KCl, 37 °C, 5 h. The product produced by T4 DNA ligase could not be purified completely by PAGE (<10% reduced product present(*)). The isolated yield of ligation product **18a** was 24% for (a) and 42% for (b).

2.5. Synthesis of spin-labeled SAM riboswitch RNAs

To further demonstrate the general applicability of the DNA-catalyzed ligation of spin-labeled RNA, we focused on the preparation of TEMPO-labeled riboswitch RNAs that may enable studies of RNA dynamics upon ligand binding by EPR spectroscopy. The first target is the 53 nt SAM-III/S_{MK} riboswitch, an analog of the S_{MK} sequence from *Enterococcus faecalis* that was optimized for determination of the crystal structure (Fig. 8a).⁴¹ We decided to split the riboswitch into two pieces of similar size and chose a ligation site within the non-conserved stem-loop region P3. In the model systems of the previous section, the spin label was installed distant from the ligation site. To employ pulsed EPR methods, it will be necessary to install two spin labels in the target RNA. Therefore we also explored a labeling position that is closer to the ligation site. In the SAM-III RNA, we chose cytidine C4 in P1 and C23 in P3 for labeling. The two 27 nt spin-labeled RNAs **20a1** and **20a2** were prepared as described above and purified by PAGE. The second fragment of 26 nt (donor substrate) was prepared by in vitro transcription. The 9DB1*-catalyzed ligation reaction was performed with equimolar concentrations of both substrates and deoxyribozyme, in 50 mM *N*-cyclohexyl-2-aminoethanesulfonic acid (CHES) buffer, pH 9.0, containing 150 mM NaCl, 2 mM KCl, and 40 mM MgCl₂, at 37 °C for 5 h. After addition of EDTA and precipitation, the nucleic acids were separated by PAGE (Fig. 8b). The ligation efficiency was similar in all three reactions, indicating that the spin labels were well tolerated at both investigated positions. The ligated RNA was isolated and characterized by CW-EPR in comparison to the non-ligated acceptor RNA **20a2** (Fig. 8c). The slightly broader spectrum of the full-length 53-mer RNA suggests reduced motion compared to the shorter unstructured 27-mer, as it would be expected upon almost doubling the size of the RNA.

As a second target, we chose the 118-mer *yitJ* SAM-I riboswitch RNA of *Bacillus subtilis* (Fig. 8d).^{42,43} The TEMPO label was introduced at position 8 of the 18-nt 5'-terminal fragment **22a**. The ligation

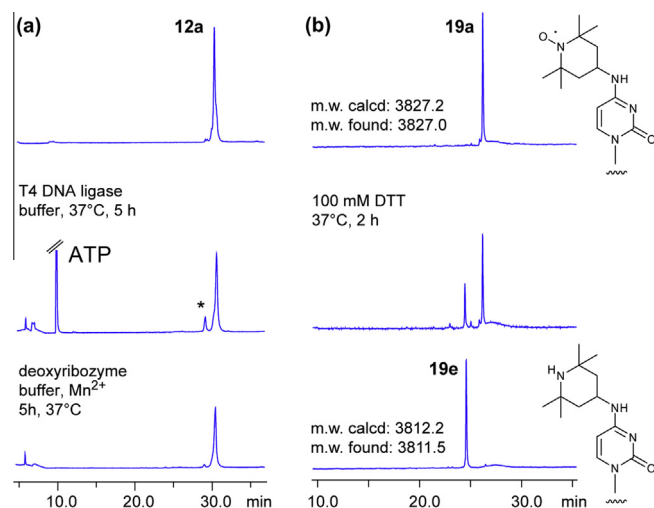


Figure 7. Examination of stability of spin-labeled RNA under ligation conditions. (a) 20-mer C^{TEMPO}-labeled RNA **12a** is incubated with T4 DNA ligase buffer (40 mM Tris-HCl pH 7.8, 10 mM MgCl₂, 10 mM DTT, 0.5 mM ATP) for 5 h at 37 °C. (b) Characterization of reduction product by comparison with authentic 2,2,6,6-tetramethylpiperidine-substituted RNA **19e**.

tion site resides within helix P2. Two 5'-triphosphorylated donor substrates were generated by in vitro transcription. RNA **23** spans nt 19–70 of the riboswitch RNA and was used as a test case to confirm the efficiency of the ligation site (Fig. S10). The 100 nt donor substrate **25** was generated by in vitro transcription from a double-stranded DNA template that was produced by polymerase extension of overlapping primers. The DNA-catalyzed ligation was performed at pH 7.5 in 50 mM 4-(2-hydroxyethyl)-1-piperazineethanesulfonic acid (HEPES) buffer in the presence of 20 mM MnCl₂. Examination of the ligation time-course at 10 μ M RNA concentration revealed good conversion and produced 70% ligated product after 3–5 h. Figure 8e displays the analysis of the ligation reaction by comparing the sample composition at the start of the ligation and after 5 h of incubation at 37 °C for the unmodified (**22**) and the TEMPO-labeled substrate **22a**. In a separate larger scale reaction, the full-length spin-labeled SAM-I riboswitch RNA was isolated in 30% yield (Fig. S11). These results pave the way for EPR-based studies of changes in local dynamics upon binding of ligands to long riboswitch RNAs.^{44,45}

3. Conclusions

In summary, we have introduced TEMPO and proxyl labels at N⁴ of cytidine and 2'-O-methylcytidine, and used the resulting spin-labeled RNA oligonucleotides as acceptor substrates in DNA-catalyzed ligation reactions for the synthesis of long spin-labeled RNA. Both TEMPO and proxyl labels are well accommodated in the major groove of RNA duplexes, as revealed by only moderate thermodynamic destabilization and the observed spectral broadening of CW-EPR signals upon hybridization to complementary strands.

Spin-labeled RNAs are suboptimal substrates for ligation by T4 DNA ligase due to the sensitivity of nitroxides to reduction. Importantly, under the conditions used for DNA-catalyzed ligation with 9DB1*, the spin label integrity was not affected. The TEMPO and proxyl groups were well tolerated at diverse positions in the acceptor strand that is generated by solid-phase synthesis using convertible nucleoside phosphoramidites. The donor strand is accessible by in vitro transcription, and is currently not directly amenable to site-specific modification using convertible nucleosides. How-

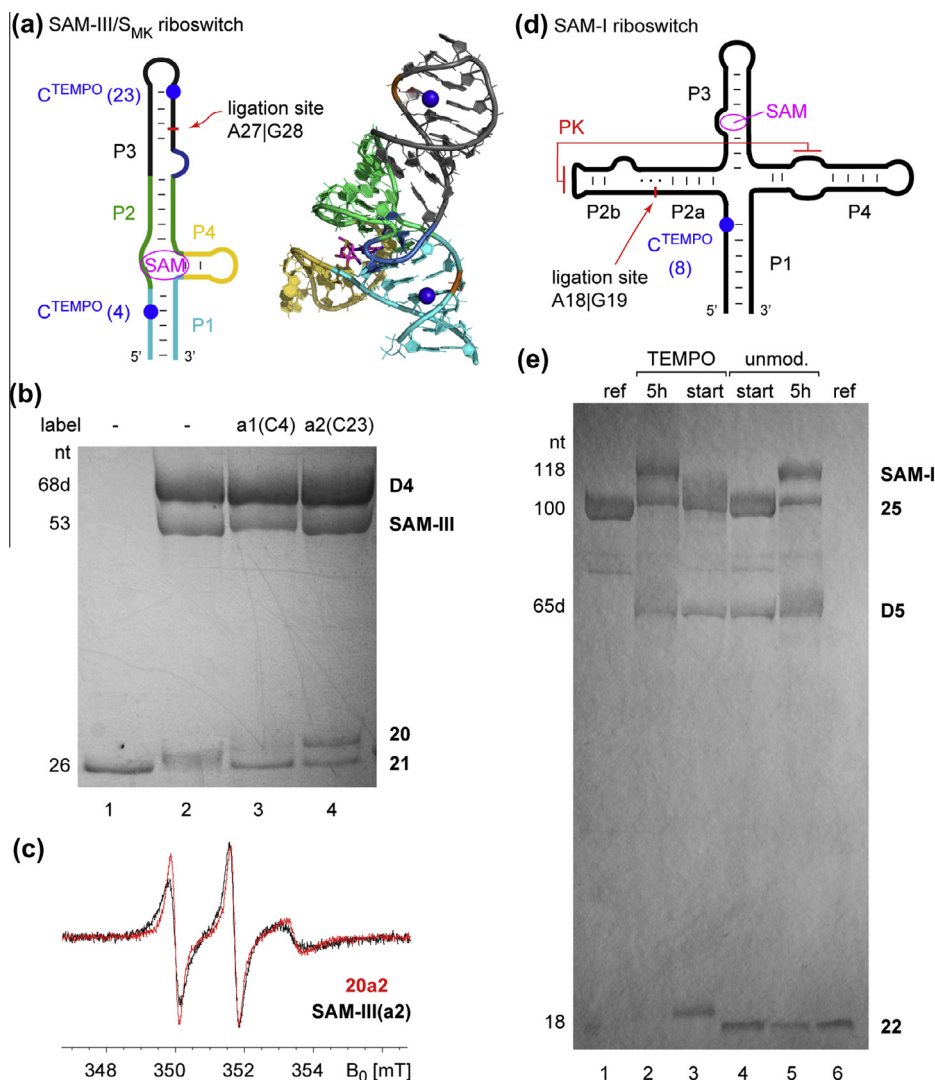


Figure 8. Synthesis of spin-labeled riboswitch RNAs. (a) fragment of SAM-III/S_{MK} riboswitch, analogous to construct used for determination of X-ray structure.⁴¹ Blue spheres in the pymol picture indicate attachment points for TEMPO (i.e., N4 of C4 and C23), (b) gel image of SAM-III ligation: lane 1. reference for donor **21**; lane 2. ligation of unmodified RNAs **20** + **21**, lane 3. TEMPO at C4: **20a1** + **21**; lane 4. TEMPO at C23: **20a2**+**21**; conditions for lanes 2–4: 15 μM RNA, 40 mM MgCl₂, pH 9.0, 37 °C, 5 h; 9DB1* deoxyribozyme D4. (c) CW-EPR spectrum of 53 nt SAM-III RNA (with TEMPO at C23) in comparison to unligated RNA **20a2** (40 μM RNA in each case). (d) Schematic depiction of *Bacillus subtilis* *yitJ* SAM-I riboswitch aptamer (118 nt);⁴³ (e) gel image of SAM-I ligation: lane 1. reference for donor substrate **25** (100 nt); ligation of spin-labeled SAM-I **22a** + **25**: lane 2: 5 h. lane 3: start; unmodified comparison **22** + **25**: lane 4: start, lane 5: 5 h; lane 6: reference for acceptor **22**; ligation conditions lanes 2–5: 15 μM RNA, 20 mM MnCl₂, pH 7.5, 37 °C, 5 h; 9DB1* deoxyribozyme D5.

ever, with recent reports of improved synthetic methods for the installation of 5'-triphosphates by solid-phase synthesis,^{46,47} functionalized and/or labeled donor substrates for 9DB1* ligation are coming into reach.

With the successful DNA-catalyzed synthesis of spin-labeled RNAs up to 118 nt in length, this work sets a new benchmark for preparative applications of deoxyribozymes. The DNA catalyst for a ligation reaction can be obtained as standard DNA oligonucleotide from commercial suppliers, just like DNA splints or primers are nowadays ordered by scientists on an almost daily basis. Simple buffers and divalent metal ions are the only other necessary ingredients. The DNA catalyst is used in stoichiometric amount with respect to the RNA substrates, and can easily be separated from the product, re-isolated and used again in another ligation experiment.

One of the advantages of EPR spectroscopy lies in the relatively small amount of sample that is required. With modern instruments and high-field techniques, EPR experiments can be performed with less than 5 μL of 50 μM spin-labeled RNA.⁴⁸ This amount is readily

obtained by the described method; ligation of spin-labeled RNA was here performed on the low nmol-scale (up to 3 nmol), but the approach is expected to be easily scalable to multi-nmols of isolated ligation product. Moreover, the application of 9DB1* on preparative scale is certainly not limited to TEMPO- and proxyl-labeled RNA, but will be useful for the synthesis of diverse labeled RNAs for spectroscopic and biochemical studies.

4. Experimental procedures

4.1. General procedures

Thin layer chromatography (TLC) was carried out using silica gel on aluminum sheets (200 μM, F-254). Compounds were visualized by UV light and staining with *p*-anisaldehyde. Flash-column chromatography was performed using ultrapure flash silica gel (230–400 mesh size, 60 Å). All moisture- and air-sensitive reactions were carried out in oven-dried glassware under an inert argon atmosphere. NMR spectra were recorded on a

400 MHz spectrometer. Commercial grade CDCl_3 was passed over basic alumina shortly before use for tritylated compounds. ^1H NMR chemical shifts are reported in reference to undeuterated residual solvent in CDCl_3 (7.26 ppm). ^{13}C NMR chemical shifts are reported in reference to solvent signal (CDCl_3 (77.16 ppm)). ^{31}P NMR chemical shifts are reported relative to 85% H_3PO_4 as an external standard.

4.2. Synthesis of convertible nucleoside phosphoramidites

4.2.1. 5'-O-(4,4'-Dimethoxytrityl)-2'-O-(triisopropylsilyl)oxymethyl- O^4 -(4-chlorophenyl)uridine (3)

5'-O-DMT-2'-O-TOM-uridine **2** was prepared from uridine in two steps as previously described.³⁶ Compound **2** (390 mg, 0.53 mmol, 1.00 equiv) was dissolved in DCM (6 mL), and DMAP (9.8 mg, 0.08 mmol, 0.15 equiv) and NEt_3 (0.66 mL, 4.79 mmol, 9.00 equiv) were added. The solution was cooled to 0 °C and 2,4,6-triisopropylbenzenesulfonyl chloride (212 mg, 0.70 mmol, 1.32 equiv) was added. The solution was stirred at 0 °C for 10 min, allowed to warm up and stirred at ambient temperature for 2 h. The reaction mixture was diluted with DCM, washed with NaHCO_3 , dried over Na_2SO_4 and evaporated under reduced pressure. The crude product was directly used for the next step. Crude 5'-O-DMT-2'-O-TOM- O^4 -trityl-uridine (532 mg) was dissolved in DCM (12 mL) and 4-chlorophenol (343 mg, 2.67 mmol, 5.00 equiv) and *N,N*-dimethylethylamine (0.87 mL, 8.00 mmol, 15.0 equiv) were added. DBU (0.08 mL, 0.53 mmol, 1.00 equiv) was added over 5 min and the resulting mixture was stirred for 90 min. The organic layer was washed with NaHCO_3 , dried over Na_2SO_4 and evaporated under reduced pressure. Purification by column chromatography on SiO_2 with 20–80% ethyl acetate in hexane (containing 2% NEt_3) yielded the desired compound **3** (423 mg, 0.50 mmol, 94%) as white foam. R_f (hexane/ethyl acetate 3:1) = 0.32; ^1H NMR (400 MHz, CDCl_3): δ (ppm) = 1.04–1.09 (m, 21 H, $(\text{CH}_3)_2\text{CH-Si}$, $(\text{CH}_3)_2\text{CH-Si}$), 3.33 (d, 1 H, $J = 8.4$ Hz, $\text{HO-C}(3')$), 3.56 (dd, 1 H, $J = 11.2$ Hz, $J = 2.3$ Hz, $\text{H-C}(5')_a$), 3.62 (dd, 1 H, $J = 11.2$ Hz, $J = 2.3$ Hz, $\text{H-C}(5')_b$), 3.81 (s, 6 H, OCH_3), 4.08 (dt, 1 H, $J = 8.9$ Hz, $J = 2.3$ Hz, $\text{H-C}(4')$), 4.22 (d, 1 H, $J = 5.0$ Hz, $\text{H-C}(2')$), 4.42 (ddd, 1 H, $J = 8.9$ Hz, $J = 8.4$ Hz, $J = 5.0$ Hz, $\text{H-C}(3')$), 5.12 (d, 1 H, $J = 4.7$ Hz, $2'\text{-OCH}_2\text{O}$), 5.27 (d, 1 H, $J = 4.7$ Hz, $2'\text{-OCH}_2\text{O}$), 5.65 (d, 1 H, $J = 7.4$ Hz, $\text{H-C}(5)$), 5.94 (s, 1 H, $\text{H-C}(1')$), 6.86 (dd, 4 H, $J = 8.6$ Hz, $J = 1.1$ Hz, DMT-H_{ar}), 7.09 (dd, 2 H, $J = 9.6$ Hz, $J = 3.2$ Hz, pCl-Ph-H_{ar}), 7.23–7.28 (m, 2 H, H_{ar}), 7.30–7.35 (m, 7 H, H_{ar}), 7.40–7.44 (m, 2 H, H_{ar}), 8.50 (d, 1 H, $J = 7.4$ Hz, $\text{H-C}(6)$); ^{13}C NMR (100 MHz, CDCl_3): δ (ppm) = 11.8 ($(\text{CH}_3)_2\text{CH-Si}$), 17.8 ($(\text{CH}_3)_2\text{CH-Si}$), 55.3 (DMT-OCH_3), 61.0 ($\text{C}(5')$), 67.6 ($\text{C}(3')$), 83.3 ($\text{C}(4')$), 83.4 ($\text{C}(2')$), 87.0 (DMT-C_q), 90.1 ($\text{C}(1')$), 90.8 ($2'\text{-OCH}_2\text{O}$), 94.8 ($\text{C}(5)$), 113.3 (DMT-C_{ar}), 123.1 (pCl-Ph-C_{ar}), 123.8, 123.9, 127.1, 128.0, 128.3, 129.6, 130.3, 131.2, 135.2, 135.5, 144.5 ($\text{C}(6)$), 144.6, 150.1, 151.3, 155.0 ($\text{C}(2)$), 158.7 (DMT-C_{ar}), 158.7 (DMT-C_{ar}), 171.2 ($\text{C}(4)$); MS (ESI) $m/z = 865.1$ [$\text{M}+\text{Na}$] $^+$.

4.2.2. 5'-O-(4,4'-Dimethoxytrityl)-2'-O-(triisopropylsilyl)oxymethyl- O^4 -(4-chlorophenyl)uridine 3'-(2-cyanoethyl-*N,N*-diisopropylphosphoramidite) (4)

5'-O-DMT-2'-O-TOM- O^4 -(4-chlorophenyl)uridine **3** (201 mg, 0.24 mmol, 1.00 equiv) was dried under high vacuum overnight and dissolved in DCM (5 mL). *N,N*-Dimethylethylamine (0.26 mL, 0.24 mmol, 1.00 equiv) and 2-cyanoethyl-*(N,N)*-diisopropylamino chlorophosphite (98.7 mg, 0.42 mmol, 1.75 equiv) were added and the solution stirred at ambient temperature for 2.5 h. A few drops of methanol were added to stop the reaction, and the organic phase was washed with NaHCO_3 , dried over Na_2SO_4 and evapo-

rated under reduced pressure. The crude product was purified by column chromatography on SiO_2 (hexane/ethyl acetate 3:1, 2% NEt_3) yielding compound **4** (159 mg, 0.15 mmol, 64%) as a white foam. R_f (hexane/ethyl acetate 3:1) = 0.39; ^1H NMR (400 MHz, CDCl_3): δ (ppm) = 1.00 (d, 12 H, $J = 6.7$ Hz, $(\text{CH}_3)_2\text{CHN}$), 1.03–1.19 (m, 54 H, $(\text{CH}_3)_2\text{CHN}$, $(\text{CH}_3)_2\text{CH}_2\text{Si}$), 2.40 (t, 2 H, $J = 6.4$ Hz, $\text{OCH}_2\text{CH}_2\text{CN-H}_a$), 2.60 (t, 1 H, $J = 6.2$ Hz, $\text{OCH}_2\text{CH}_2\text{CN-H}_b$, diastereomer 1), 2.61 (t, 1 H, $J = 6.2$ Hz, $\text{OCH}_2\text{CH}_2\text{CN-H}_b$, diastereomer 2), 3.46 (td, 2 H, $J = 10.6$ Hz, $J = 2.5$ Hz, $\text{H-C}(5')_a$), 3.52–3.75 (m, 8 H, $\text{H-C}(5')_b$, $2 \times (\text{CH}_3)_2\text{CH-N}$, $\text{OCH}_2\text{CH}_2\text{CN-H}_a$), 3.81 (s, 12 H, OMe), 3.88–3.96 (m, 2 H, $\text{OCH}_2\text{CH}_2\text{CN-H}_b$), 4.25–4.32 (m, 4 H, $\text{H-C}(2')$, $\text{H-C}(4')$), 4.46 (ddd, 1 H, $J = 9.5$ Hz, $J = 8.0$ Hz, $J = 4.9$ Hz, $\text{H-C}(3')$, diastereomer 1), 4.57 (ddd, 1 H, $J = 9.5$ Hz, $J = 8.0$ Hz, $J = 4.9$ Hz, $\text{H-C}(3')$, diastereomer 2), 5.13 (d, 1 H, $J = 4.2$ Hz, $2'\text{-OCH}_2\text{-H}_a$, diastereomer 1), 5.14 (d, 1 H, $J = 4.2$ Hz, $2'\text{-OCH}_2\text{-H}_a$, diastereomer 2), 5.22 (d, 1 H, $J = 4.2$ Hz, $2'\text{-OCH}_2\text{-H}_b$, diastereomer 1), 5.23 (d, 1 H, $J = 4.2$ Hz, $2'\text{-OCH}_2\text{-H}_b$, diastereomer 2), 5.56 (d, 1 H, $J = 7.3$ Hz, $\text{H-C}(5)$, diastereomer 1), 5.62 (d, 1 H, $J = 7.3$ Hz, $\text{H-C}(5)$, diastereomer 2), 6.12 (s, 2 H, $\text{H-C}(1')$), 6.83–6.88 (m, 8 H, DMT-H_{ar}), 7.06–7.09 (m, 4 H, pCl-Ph-H_{ar}), 7.25–7.34 (m, 18 H, H_{ar}), 7.39–7.45 (m, 4 H, H_{ar}), 8.42 (d, 1 H, $J = 7.4$ Hz, $\text{H-C}(6)$, diastereomer 1), 8.49 (d, 1 H, $J = 7.4$ Hz, $\text{H-C}(6)$, diastereomer 2); ^{31}P NMR (162 MHz, CDCl_3): δ (ppm) = 149.9 (s); MS (ESI) $m/z = 1065$ [$\text{M}+\text{Na}$] $^+$.

4.2.3. 5'-O-(4,4'-Dimethoxytrityl)-2'-O-methyluridine (7)

5'-O-DMT-2,2'-O-anhydrouridine (**6**) was prepared in two steps from uridine as previously described.^{37,38} The conversion to 5'-O-DMT-2'-O-methyluridine was performed in analogy to earlier reports.^{39,40} Magnesium methoxide was freshly prepared by heating Mg (0.5 g) in methanol (50 mL) at 60 °C for 2 h, evaporation of excess methanol and drying of the gray powder under vacuum. Dried $\text{Mg}(\text{OCH}_3)_2$ (740 mg, 8.57 mmol, 6.00 equiv) was added to a suspension of compound **6** (750 mg, 1.42 mmol, 1.00 equiv) in DMF (20 mL) and the mixture was heated to 100 °C for 2 h. A clear solution was obtained. The solvent was evaporated and the residue was taken up in ethyl acetate. The organic layer was washed with NaHCO_3 and water, dried over Na_2SO_4 and evaporated under reduced pressure. The crude product was purified by column chromatography on SiO_2 with 2–4% methanol in DCM to give compound **7** (510 mg, 0.91 mmol, 64%) as white solid. ^1H NMR (400 MHz, CDCl_3): δ (ppm) = 3.54–3.57 (m, 2 H, $\text{H-C}(5')$), 3.65 (s, 3 H, $2'\text{-OCH}_3$), 3.79–3.80 (m, 7 H, $\text{H-C}(2')$, DMT-OCH_3), 3.98–4.01 (m, 1 H, $\text{H-C}(4')$), 4.45–4.50 (m, 1 H, $\text{H-C}(3')$), 5.26 (d, 1 H, $J = 8.1$ Hz, $\text{H-C}(5)$), 5.97 (s, 1 H, $\text{H-C}(1')$), 6.82–6.86 (m, 4 H, DMT-H_{ar}), 7.24–7.39 (m, 9 H, DMT-H_{ar}), 8.03 (d, 1 H, $J = 8.1$ Hz, $\text{H-C}(6)$); MS (ESI): $m/z = 583.1$ [$\text{M}+\text{Na}$] $^+$.

4.2.4. 5'-O-(4,4'-Dimethoxytrityl)- O^4 -(4-chlorophenyl)-2'-O-methyluridine (8)

5'-O-DMT-2'-O-methyluridine (**7**) (120 mg, 0.26 mmol, 1.00 equiv) was dissolved in DCM (1 mL), triethylamine (0.20 mL) and DMAP (120 mg, 0.26 mmol, 1.00 equiv) were added at 0 °C and the mixture was stirred at 0 °C for 15 min. 2,4,6-triisopropylbenzenesulfonyl chloride (133 mg, 0.44 mmol, 1.70 equiv) was added and stirring was continued for 30 min at 0 °C and another 2 h at ambient temperature. The reaction mixture was diluted with DCM and the organic layer washed with water and NaHCO_3 , dried over Na_2SO_4 and evaporated under reduced pressure. The residue was taken up in DCM (2 mL) and *N,N*-dimethylethylamine (133 mg, 0.44 mmol, 1.70 equiv) and 4-chlorophenol (133 mg, 0.44 mmol, 1.70 equiv) were added under vigorous stirring. After 20 min, DBU (39.6 mg, 0.26 mmol, 1.00 equiv) was added and stirring was continued for 3 h. The solvent was evaporated under reduced pressure and the crude product was purified by column chromatography on SiO_2 with 2–5% ethyl acetate in hexane to give target compound **8** (107 mg,

0.16 mmol, 62%) as white solid. R_f (hexane/ethyl acetate 1:1) = 0.18; ^1H NMR (400 MHz, CDCl_3): δ (ppm) = 2.56 (d, 1 H, $J = 10.5$ Hz, HO-C(3')), 3.53–3.65 (m, 3 H, H-C(5'), H-C(2')), 3.72 (s, 3 H, 2'-OCH₃), 3.81 (s, 6 H, OCH₃), 3.99–4.04 (m, 1 H, H-C(4')), 4.42–4.51 (m, 1 H, H-C(3')), 5.64 (d, 1 H, $J = 7.3$ Hz, H-C(5)), 5.98 (s, 1 H, H C(1')), 6.84–6.88 (m, 4 H, DMT- H_{ar}), 7.06–7.10 (m, 2 H, pCl-Ph- H_{ar}), 7.28–7.43 (m, 11 H, DMT- H_{ar} , pCl-Ph- H_{ar}), 8.54 (d, 1 H, $J = 7.3$ Hz, H-C(6)). ^{13}C NMR (100 MHz, CDCl_3): δ (ppm) = 55.7 (DMT-OCH₃), 59.3 (2'-OCH₃), 61.1 (C(5')), 68.1 (C(3')), 83.5 (C(2')), 84.2 (C(4')), 88.7 (C_q), 95.2 (C(1')), 113.5, 113.7 (DMT-C_{ar}), 123.5, 127.5, 128.1, 128.2, 128.3, 128.6, 129.5, 129.9, 130.5, 130.6, 135.5, 135.7, 144.7, 144.9, 145.9, 159.0, 171.5 (C_{ar}). MS (ESI): m/z = 693.2 [M+Na]⁺, 709.1 [M+K]⁺.

4.2.5. 5'-O-(4',4'-Dimethoxytrityl)-O⁴-(4-chlorophenyl)-2'-O-methyluridine 3'-(2-cyanoethyl)-N,N-diisopropylphosphoramidite (9)

5'-O-DMT-O⁴-(4-chlorophenyl)-2'-O-methyluridine (8) (93.6 mg, 0.14 mmol, 1.00 equiv) was dried under high vacuum overnight and dissolved in DCE (2.5 mL). *N,N*-Dimethylethylamine (109 mg, 1.40 mmol, 10.0 equiv) and 2-cyanoethyl-(*N,N*-diisopropylamino) chlorophosphite (57.8 mg, 0.24 mmol, 1.75 equiv) were added and the mixture stirred for 2 h. The reaction was stopped by addition of a few drops of methanol, the organic layer was diluted with DCM and washed with NaHCO₃ and water, dried over Na₂SO₄ and evaporated under reduced pressure. The crude product was purified by column chromatography on SiO₂ with 20–50% ethyl acetate in hexane (containing 2% NEt₃), to yield target compound 9 (80.4 mg, 0.09 mmol, 66%) as white foam. R_f (hexane/ethyl acetate 1:1) = 0.57; ^1H NMR (400 MHz, CDCl_3): δ (ppm) = 0.98 (d, 6 H, $J = 6.8$ Hz, (CH₃)₂CHN), 1.11–1.26 (m, 18 H, (CH₃)₂CHN), 2.39 (t, 2 H, $J = 6.0$ Hz, CH₂CH₂CN- H_a), 2.60 (t, 2 H, $J = 6.0$ Hz, CH₂CH₂CN- H_b), 3.42–3.88 (m, 14 H, H-C(2')), 2 × H-C(5'), ((CH₃)₂CH)₂N, 2 × CH₂CH₂CN), 3.63 (s, 6 H, 2'-OCH₃), 3.78–3.79 (m, 12 H, OCH₃), 4.22–4.26 (m, 2 H, H-C(4')), 4.43 (td, 1 H, $J = 9.0$ Hz, $J = 4.7$ Hz, H-C(3') diastereomer 1), 4.61 (td, 1 H, $J = 9.0$ Hz, $J = 4.7$ Hz, H-C(3') diastereomer 2), 4.48 (d, 1 H, $J = 7.4$ Hz, H-C(5), diastereomer 1), 5.54 (d, 1 H, $J = 7.4$ Hz, H-C(5), diastereomer 2), 5.96 (s, 1 H, H-C(1'), diastereomer 1), 5.99 (s, 1 H, H-C(1'), diastereomer 2), 6.80–6.86 (m, 8 H, DMT- H_{ar}), 7.05–7.09 (m, 4 H, pCl-Ph- H_{ar}), 7.23–7.43 (m, 22 H, H_{ar}), 8.53 (d, 1 H, $J = 7.4$ Hz, H-C(6), diastereomer 1), 8.59 (d, 1 H, $J = 7.4$ Hz, H-C(6), diastereomer 2); ^{31}P NMR (162 MHz, CDCl_3): δ (ppm) = 150.1 (s, diastereomer 1), 150.5 (s, diastereomer 2); MS (ESI): m/z = 893.3 [M+Na]⁺.

4.3. Synthesis of spin-labeled RNA

RNA solid-phase syntheses were performed on a Pharmacia Gene Assembler Plus, using 0.7 μmol polystyrene custom primer support from GE Healthcare. 2'-O-TOM-protected ribonucleoside phosphoramidites were used for all unmodified RNA nucleotide positions (100 mM in CH₃CN). Convertible nucleoside phosphoramidites were dried over-night under high vacuum and then dissolved in dry CH₃CN. The solutions were dried over molecular sieves for several hours before installation on the gene assembler. *S*-Benzylthiotetrazole (BTT) (250 mM in CH₃CN) was used as activator; coupling time was 4 min. Detritylation, capping and oxidation was performed under standard conditions.

Solid support containing the fully protected RNA (ca. 0.3 μmol) was incubated with 4-amino-TEMPO or 3-amino-proxyl (100 μL , 2 M in methanol) for 24–48 h at 42–55 °C. For all reactions with 3-amino-proxyl and for all RNAs longer than 15 nt, MeNH₂ in H₂O (500 μL , 8 M) or NH₄OH (500 μL , 25% aq) was added and incubated in a tightly closed vial for 2–5 h (37 °C for MeNH₂, 55 °C for NH₄OH). The solid support was removed by filtration, and the sol-

vents were evaporated. The residue was dissolved in a solution of TBAF in THF (500 μL , 1 M) and incubated at room temperature for 8–16 h. Aqueous buffer (500 μL , 1 M Tris-HCl pH 8.0) was added, and THF was removed under reduced pressure before desalting on HiTrap desalting columns (3 × 5 mL). The aqueous eluate was concentrated and the crude product stored at –20 °C.

Anion exchange HPLC was performed on Dionex DNA-Pac PA200 column, 4 × 250 mm at 70 °C. Buffer A: 25 mM Tris-HCl, pH 8.0, 6 M urea. Buffer B: same as A + 0.5 M NaClO₄.

PAGE purification was performed on 15% or 20% polyacrylamide gels (acrylamide:bisacrylamide 19:1) in 1 × TBE buffer. Gel dimensions: 0.7 × 200 × 320 mm. Samples were loaded with formamide loading buffer (containing bromophenol blue and xylene cyanol as dye markers) and run at 35 W. Bands were detected by UV shadowing and extracted by the 'crush and soak' method using TEN buffer as previously described.³⁵

4.4. In vitro transcription of donor fragments

In vitro transcription was performed as in our previous reports³⁵ with T7 RNA polymerase and synthetic DNA templates (1 μM) using 4 mM of each NTP in 40 mM Tris-HCl, pH 8.0, 30 mM MgCl₂, 10 mM DTT, and 2 mM spermidine at 37 °C for 5 h.

4.5. General procedure for DNA-catalyzed ligation of RNA fragments

Spin-labeled or unmodified acceptor RNA, in vitro transcribed donor RNA, and 9DB1* DNA were combined in equimolar ratio and annealed in 25 mM HEPES, pH 7.5, 15 mM NaCl, 0.1 mM EDTA by heating to 95 °C for 2 min and slow cooling to room temperature. The reaction buffer and divalent metal ions were added from 5 × concentrated stock solutions. The final concentrations were 50 mM HEPES, pH 7.5, 150 mM NaCl, 2 mM KCl, 20 mM MnCl₂ or 50 mM CHES, pH 9.0, 150 mM NaCl, 2 mM KCl, 40 mM MgCl₂. Ligation reactions were performed on a scale of 150 pmol up to 3 nmol per substrate at a final concentration of each strand at 15 μM . The ligation mixture was incubated at 37 °C for 5 h (or at 25 °C for 12 h for the shortest substrates). EDTA was added (50 mM) and the RNA and DNA strands were precipitated by addition of cold ethanol (3 vol). Reactions were analyzed, and products were isolated by anion exchange HPLC or PAGE.

4.6. Ligation of RNA by T4 DNA ligase

Equimolar amounts of acceptor RNA, 5'-phosphorylated donor RNA and DNA splint were annealed by heating to 95 °C for 2 min and slow cooling to ambient temperature (final RNA concentration was 15 μM of each strand). T4 DNA ligase buffer (final concentration 40 mM Tris-HCl, pH 7.8, 10 mM MgCl₂, 10 mM DTT, 0.5 mM ATP) and T4 DNA ligase (final concentration 0.5 U/ μL) were added, and the reaction mixture was incubated at 37 °C for 6–12 h and analyzed by anion exchange HPLC or PAGE.

4.7. Kinetic assays of DNA-catalyzed ligation

Assays of 9DB1*-catalyzed ligation kinetics were performed under single-turnover conditions with 5'-³²P-labeled acceptor RNA as described.³⁵ Time points were taken up to 5 h, and samples were analyzed by PAGE. Gels were dried, exposed to a PhosphorImager screen, and imaged with a PhosphorImager. The ligation yield was determined by volume integration and the data were fit to the equation $\text{yield} = Y^*(1 - e^{-kt})$, where $k = k_{\text{obs}}$ and $Y = \text{final yield}$.

4.8. Thermal melting experiments

RNA duplexes were prepared at 1–25 μM in 10 mM potassium phosphate buffer, pH 7.0, 150 mM NaCl. Melting curves were monitored in quartz cuvettes of 1 cm or 0.1 cm path length at 250, 260, 270, and 280 nm on a Cary 100 UV spectrophotometer (Varian Inc.) equipped with a multiple cell holder and a Peltier temperature-controller. Two full heating and cooling cycles (4 ramps) were collected with a heating/cooling rate of 0.7 $^{\circ}\text{C}/\text{min}$. Hyperchromicity at 250 nm was calculated, and the T_m was determined at the maximum of the first derivative of the hyperchromicity curve. Thermodynamic parameters were obtained by analysis of $\ln(c_T)$ versus $1/T_m$, with c_T calculated from A^{260} at T_m .

4.9. EPR experiments

CW-EPR spectra were acquired on a Bruker EMX spectrometer at 22 $^{\circ}\text{C}$, using 100 kHz modulation frequency, 0.8 G modulation amplitude, and 2.0 mW microwave power. Measurements were taken in quartz capillaries containing 40 μM or 200 μM spin-labeled RNA in 2.5 mM potassium phosphate buffer, pH 7.0, 30 mM NaCl. The duplex samples contained 1.5 equiv of the unlabeled complementary strand. Double strands were annealed by heating to 95 $^{\circ}\text{C}$ for 2 min and slow cooling to room temperature before transfer to the capillary.

Acknowledgments

We gratefully acknowledge financial support by the DFG (IRTG 1422 and GSC 226/1) and the Max Planck Society. A.O. thanks the Beilstein foundation for a research scholarship. We thank Professor Dr. Marina Bennati, MPIIbpc for access to the Bruker EMX spectrometer, and Drs. Soraya Pornsuwan and Igor Tkach for assistance with EPR data acquisition. Uwe Plessmann (Facility for Bioanalytical Mass spectrometry) and Jürgen Bienert (Facility for Synthetic Chemistry) are acknowledged for recording MS and NMR spectra.

Supplementary data

Supplementary data associated with this article can be found, in the online version, at <http://dx.doi.org/10.1016/j.bmc.2013.04.007>.

References and notes

- Gesteland, R. F.; Cech, T. R.; Atkins, J. F. *The RNA World*, 3rd ed.; CSHL Press, 2006.
- Wachowius, F.; Höbartner, C. *ChemBioChem* **2010**, *11*, 469.
- Solomatin, S.; Herschlag, D. *Methods Enzymol.* **2009**, *469*, 47.
- Shelke, S. A.; Sigurdsson, S. T. *Eur. J. Org. Chem.* **2012**, 2291.
- Piton, N.; Mu, Y.; Stock, G.; Prisner, T. F.; Schiemann, O.; Engels, J. W. *Nucleic Acids Res.* **2007**, *35*, 3128.
- Qin, P. Z.; Haworth, I. S.; Cai, Q.; Kusnetzow, A. K.; Grant, G. P. G.; Price, E. A.; Sowa, G. Z.; Popova, A.; Herreros, B.; He, H. *Nat. Protoc.* **2007**, *2*, 2354.
- Allerson, C. R.; Chen, S. L.; Verdine, G. L. *J. Am. Chem. Soc.* **1997**, *119*, 7423.
- Sicoli, G.; Wachowius, F.; Bennati, M.; Höbartner, C. *Angew. Chem., Int. Ed.* **2010**, *49*, 6443.
- Höbartner, C.; Sicoli, G.; Wachowius, F.; Gophane, D. B.; Sigurdsson, S. T. *J. Org. Chem.* **2012**, *77*, 7749.
- Roth, A.; Breaker, R. R. *Annu. Rev. Biochem.* **2009**, *78*, 305.
- Serganov, A.; Nudler, E. *Cell* **2013**, *152*, 17.
- Haller, A.; Souliere, M. F.; Micura, R. *Acc. Chem. Res.* **2011**, *44*, 1339.
- Frilander, M. J.; Turunen, J. J. In *Handbook of RNA Biochemistry*; Hartmann, R. K., Bindereif, A., Schön, A., Westhof, E., Eds.; Wiley-VCH, 2008; p 36.
- Haller, A.; Altman, R. B.; Souliere, M. F.; Blanchard, S. C.; Micura, R. *Proc. Natl. Acad. Sci. U.S.A.* **2013**, *110*, 4188.
- Haller, A.; Rieder, U.; Aigner, M.; Blanchard, S. C.; Micura, R. *Nat. Chem. Biol.* **2011**, *7*, 393.
- Rieder, R.; Höbartner, C.; Micura, R. *Methods Mol. Biol.* **2009**, *540*, 15.
- Lang, K.; Micura, R. *Nat. Protoc.* **2008**, *3*, 1457.
- Brenner, M. D.; Scanlan, M. S.; Nahas, M. K.; Ha, T.; Silverman, S. K. *Biochemistry* **2010**, *49*, 1596.
- Moore, M. J.; Sharp, P. A. *Science* **1992**, *256*, 992.
- Silverman, S. K.; Cech, T. R. *Biochemistry* **1999**, *38*, 14224.
- Höbartner, C.; Silverman, S. K. *Angew. Chem., Int. Ed.* **2005**, *44*, 7305.
- Dönmez, G.; Hartmuth, K.; Kastner, B.; Will, C. L.; Lührmann, R. *Mol. Cell* **2007**, *25*, 399.
- Getz, E. B.; Xiao, M.; Chakrabarty, T.; Cooke, R.; Selvin, P. R. *Anal. Biochem.* **1999**, *273*, 73.
- Hyodo, F.; Matsumoto, K.; Matsumoto, A.; Mitchell, J. B.; Krishna, M. C. *Cancer Res.* **2006**, *66*, 9921.
- Paletta, J. T.; Pink, M.; Foley, B.; Rajca, S.; Rajca, A. *Org. Lett.* **2012**, *14*, 5322.
- Marx, L.; Chiarelli, R.; Guiberteau, T.; Rassat, A. *J. Chem. Soc., Perkin Trans. 1* **2000**, 1181.
- Krstic, I.; Hänsel, R.; Romainczyk, O.; Engels, J. W.; Dötsch, V.; Prisner, T. F. *Angew. Chem., Int. Ed.* **2011**, *50*, 5070.
- Azarkh, M.; Singh, V.; Okle, O.; Seemann, I. T.; Dietrich, D. R.; Hartig, J. S.; Drescher, M. *Nat. Protoc.* **2013**, *8*, 131.
- Tkach, I.; Sicoli, G.; Höbartner, C.; Bennati, M. *J. Magn. Reson.* **2011**, *209*, 341.
- Tkach, I.; Pornsuwan, S.; Höbartner, C.; Wachowius, F.; Sigurdsson, S. T.; Baranova, T. Y.; Diederichsen, U.; Sicoli, G.; Bennati, M. *Phys. Chem. Chem. Phys.* **2013**, *15*, 3433.
- Egli, M.; Pallan, P. S. *Annu. Rev. Biophys. Biomol. Struct.* **2007**, *36*, 281.
- Schlosser, K.; Li, Y. *Chem. Biol.* **2009**, *16*, 311.
- Höbartner, C.; Pradeepkumar, P. I. In *New Strategies in Chemical Synthesis and Catalysis*; Pignataro, B., Ed.; Wiley-VCH, 2012; p 129.
- Purtha, W. E.; Coppins, R. L.; Smalley, M. K.; Silverman, S. K. *J. Am. Chem. Soc.* **2005**, *127*, 13124.
- Wachowius, F.; Javadi-Zarnaghi, F.; Höbartner, C. *Angew. Chem., Int. Ed.* **2010**, *49*, 8504.
- Pitsch, S.; Weiss, P. A.; Jenny, L.; Stutz, A.; Wu, X. *Helv. Chim. Acta* **2001**, *84*, 3773.
- McGee, D. P.; Vaughn-Settle, A.; Vargeese, C.; Zhai, Y. *J. Org. Chem.* **1996**, *61*, 781.
- Höbartner, C.; Micura, R. *J. Am. Chem. Soc.* **2004**, *126*, 1141.
- McGee, D. P. C.; Zhai, Y. S. *Nucleosides Nucleotides* **1996**, *15*, 1797.
- Kloiber, K.; Spitzer, R.; Tollinger, M.; Konrat, R.; Kreutz, C. *Nucleic Acids Res.* **2011**, *39*, 4340.
- Lu, C.; Smith, A. M.; Fuchs, R. T.; Ding, F.; Rajashankar, K.; Henkin, T. M.; Ke, A. *Nat. Struct. Mol. Biol.* **2008**, *15*, 1076.
- Heppell, B.; Lafontaine, D. A. *Biochemistry* **2008**, *47*, 1490.
- Heppell, B.; Blouin, S.; Dussault, A. M.; Mulhbach, J.; Ennifar, E.; Penedo, J. C.; Lafontaine, D. A. *Nat. Chem. Biol.* **2011**, *7*, 384.
- Wunnicke, D.; Strohbach, D.; Weigand, J. E.; Appel, B.; Feresin, E.; Suess, B.; Müller, S.; Steinhoff, H.-J. *RNA* **2011**, *17*, 182.
- Krstic, I.; Frolow, O.; Sezer, D.; Endeward, B.; Weigand, J. E.; Suess, B.; Engels, J. W.; Prisner, T. F. *J. Am. Chem. Soc.* **2010**, *132*, 1454.
- Zlatev, I.; Lackey, J. G.; Zhang, L.; Dell, A.; McRae, K.; Shaikh, S.; Duncan, R. G.; Rajeev, K. G.; Manoharan, M. *Bioorg. Med. Chem.* **2013**, *21*, 722.
- Zlatev, I.; Lavergne, T.; Debart, F.; Vasseur, J. J.; Manoharan, M.; Morvan, F. *Org. Lett.* **2010**, *12*, 2190.
- Nguyen, P.; Qin, P. Z. *Wiley Interdiscip. Rev. RNA* **2012**, *3*, 62.